Proceedings of ASME Turbo Expo 2011
GT2011
June 6-10, 2011, Vancouver, British Columbia, Canada

GT2011-45725

Stall inception, evolution and control in a low speed axial fan with variable pitch in motion

Stefano BIANCHI [1], Alessandro CORSINI [1], Luca MAZZUCCO [1], Lucilla MONTELEONE [1],
Anthony G. SHEARD [2]

[1] Dipartimento di Ingegneria Meccanica e Aerospaziale
Sapienza University of Rome
Via Eudossiana, 18
I-00184 Rome, Italy

[2] Fläkt Woods Limited
Axial Way, Colchester
CO4 5AR UK

ABSTRACT

Obtaining the right pitch in turbomachinery blading is crucial to efficient and successful operations. Engineers adjust the rotor's pitch angle to control the production or absorption of power. Even for low speed fans this is a promising tool. This paper focuses on a low speed axial fan's inception and the evolution of the flow instabilities in the tip region which drive the stall onset.

The authors conducted an experimental study to investigate the inception patterns of rotating stall evolution at different rotor blade stagger-angle settings with the aim of extending the stable operating range. The authors drove the fan to stall at the design stagger-angle setting and then operated the variable pitch mechanism in order to recover the unstable operation. They measured pressure fluctuations in the tip region of the low-speed axial-flow fan using a variable pitch in motion mechanism, with flush mounted probes. The authors studied the flow mechanisms for spike and modal stall inceptions in this low-speed axial-flow fan which showed relatively small tip clearance. The authors cross-correlated the pressure fluctuations and analysed the cross-spectra in order to clarify blade pitch, end-wall flow, and tip-leakage flow influences on stall inception during the transient at the rotor blades' different stagger-angle settings.

The authors observed a rotating instability near the maximum pressure-rise point at both design and low stagger-angle settings. The stall inception patterns were a spike type at the design stagger-angle setting and a modal type at the low stagger-angle setting as a result of the interaction between the incoming flow, tip-leakage flow and end-wall backflow.

INTRODUCTION

The current trend toward increased pressure rise and blade aerodynamic loading reduces the stable operating range of fans and compressors which are limited by the occurrence of aerodynamic instabilities when throttling the flow rate. Researchers have studied the detection and analysis of these different forms of aerodynamic instability for several decades. Numerous studies have clarified the problem of rotating stall of axial flow compressors and focus on multi-stage machines [1 - 3]. The earlier work of Emmons [4] was one of the first attempts to describe the mechanism underlying the propagation of rotating stall.

According to Gravdahl & Egeland [5], two main types of aerodynamic flow instability in compressors exist: (i) 'rotating stall' (in which regions of reversed flow occur locally) and (ii) 'surge' (which is characterised by periodic backflow over the entire annulus involving violent oscillations in the compression system).

'Rotating stall' is a mechanism by which the rotor adapts to a reduction in flow rate. This results in circumferentially non-uniform flow patterns rotating in the annulus. In reviewing the evolution of rotating stall, Cumpsty [6] noted that the drop in overall performance can occur as a so-called 'progressive stall' or an 'abrupt stall'. Engineers usually associated the former with a part-span stall which results in a small performance drop, whereas they associate the latter with a full-span stall and a large drop in performance. Notably, the part-span rotating stall occurs typically in single blade rows [6] and usually leads to more complex disturbances in single-rotor or stage machines than in multi-stage compressors [3].

All of these forms of instability place considerable mechanical stress on the rotors involved, which can eventually lead to mechanical failure. Strain gauge measurements on axial compressors [7] and fans [8] have reported bending stress in vanes exceeding stable operation by a factor of five and seven respectively under 'rotating stall' conditions. This leads to rapid fatigue blade failure. In contrast, a 'surge' can lead to an increased magnitude of bending stress enough to cause a mechanical failure during the surge event itself.

The mechanical stress on axial-fan blades caused by stalled operations can be higher in the case of industrial fans intended for high-temperature operations such as those used in tunnel-emergency ventilation systems [9]. To ensure reliable emergency operation, both the EN12101-3 [10] and ISO 21927-3 [11] standards require fans to have a larger tip gap (between the blades and the casing). However, although such an increased tip gap has a beneficial effect in facilitating a fan's emergency operation, it also has a detrimental effect on the fan's aerodynamic and aero-acoustic performance during routine operation.

Several studies have suggested that some features of the tip flows of both compressors and axial fans (low-speed and high-speed) are directly responsible for the generation of short wave-length disturbances (also called 'spikes' or 'pips') that cause the inception of localised part-span stall cells [12-15]. Researchers have correlated this inception mechanism with a modification of the noise signal in the casing region [6]. Other scholars have utilised an array of azimuthally distributed probes in an attempt to link the rotating unsteady patterns of centrifugal pumps and compressors to their acoustic signatures [16, 18]. Similarly, Kameier and Neise [19] established a link between tip-clearance noise and associated blade-tip flow instabilities in axial turbo-machinery by correlating rotating source and vortex mechanisms with rotating stall cells.

An analysis of the background literature suggested that a potential key to stability control and performance improvement could come from an often unappreciated aspect of turbo-machinery design: pitch. Active pitch control has the potential to interrupt the stall development and facilitate its recovery, and is therefore worthy of study.

In the early 1970's, General Electric produced proposals for a variable pitch in motion system for turbofan engines [20], while this technology is of common use in low speed industrial fan applications in order to improve operating range [21]. Recently, Langston [22] highlighted how this feature will be of interest again for reducing the fuel consumption in high by-pass turbofans.

The present research addresses the basic issue of the detection of stall precursors by analysing casing pressure signals upstream of an axial fan rotor. This paper establishes the stall characteristics of a low-speed fan using flush-mounted microphones placed at two azimuthal positions around the casing. The authors collected pressure data from these positions, then processed them to establish during the fan throttling regions: (i) stable aerodynamic operation, (ii) stall incipience and (iii) rotating stall. The variable pitch in motion system is used to recover from the stall and the authors analysed the repeated pressure data in order to qualify the fan behaviour under these conditions. The authors established spatial and temporal correlations between rotating instabilities which facilitated a full analysis of stall inception and recovery.

NOMENCLATURE

Latin letters

BPF	blade passing frequency (Hz)
f	signal frequency (Hz)
NR	Nyquist rate (Hz)
t	time [s]
U_{tip}	tip speed (m/s)
VPIM	variable pitch in motion system

Greek letters

η_{tot}	efficiency based on total pressure rise
θ	azimuthal position of the microphone

EXPERIMENTAL FACILITY

Fan

Table 1 shows the specifications for the axial fan in this study, tested in the Fläkt Woods test facility in Växjö (Sweden).

Table 1 Fan data

Nominal speed	700 rpm
Tip speed	55.13 m/s
Nominal work pressure	350 – 400 Pa
Nominal flow rate	12 – 14 m^3/s
Design efficiency, η_{tot}	0.92
Tip diameter	1500 mm
Blade heigth	450 mm
Blade chord at the tip	105 mm
Hub pitch angle	80°- 40°
Tip gap (% of blade chord at tip)	1.3%
Blade count	18
Average solidity	0.6

The 18 blade fan was equipped with a mechanism for varying the blade-pitch angle during the rotor spinning, called Variable Pitch in Motion (VPIM). The original goal of the VPIM in such a fan family, intended for induced draft operation in power plant, is to control the aerodynamic performance in a wide operating area to customise the load, the airflow and the stalling properties.

Clearance between the blade tips and the casing ranged between 1.3% and 2% of chord at tip, in the pitch angle interval operated during the test. The single-parameter blade sections were highly twisted C4 profile airfoils.

The VPIM system, in the spinner cavity, consisted of two remotely controlled oil-dynamic actuators, which drove a ring to change simultaneously the blades' pitch angle with a speed of about 1,5°/s.

Test rig facility

The authors conducted the tests at the Fläkt Woods AB test facility in Växjö, designed to comply with the ISO 5801:2007 standard, equivalent to the BS 848 Pt.1 standard [24 - 25]. The authors operated the fan in a custom-built casing made from cast and machined steel rings. The rig was driven by a 270-kW, direct coupled-induction 400-Volt (AC), 3-phase. The motor drives the rotor at a constant speed of 700 rpm, under inverter.

Table 2 Fan Test-rig specification at Flakt Woods Växjö

Mode	*Length (m)*	*Power (kW)*	*D (m)*	*rpm*	*T (°C)*
Stand-alone	50	350	4	-	-
Thrust	-	350	1.6	-	-
Spin testing	-	810	4	5000	-
High T.	6	350	3.6	-	400

The blade tip speed was 55.13 m/s. At this tip speed the blade-passing frequency (BPF) for all the tested configurations was 210 Hz.

temperature, pressure and air-speed, then discharged the airflow from the throttling valve.

Figure 1 shows the sketch of the test-rig facility, whilst Table 2 and Table 3 summarise the main characteristics of the test facility and the plenum chamber.

The authors measured the fan performance in accordance with the ISO 5801:2007 standard [24]. By throttling downstream from the fan rotor, they produced the aerodynamic instabilities of interest. During the volume-flow throttling, the fan remained in rotating stall without going into surge, irrespective of the rotor speed. The rotor's aerodynamic load and the downstream plenum geometry ensured that the system could not develop a counter-pressure able to induce a surge. As such, the value of the B parameter for the plenum system was 0,15, well below Greitzer's suggested threshold value [26] for axial compressor rigs.

Table 3 Pressure chamber characteristics

volume flow rate (m^3/s)	*static pressure (Pa)*	*width (m)*	*Length (m)*	*height (m)*
50	50000	4	4	9

Test conditions

Figure 2 shows the fan's performance map at full-speed operation for three different pitch angles.

The fan chart was obtained running the fan rotor to unstable operation by gradually throttling downstream.

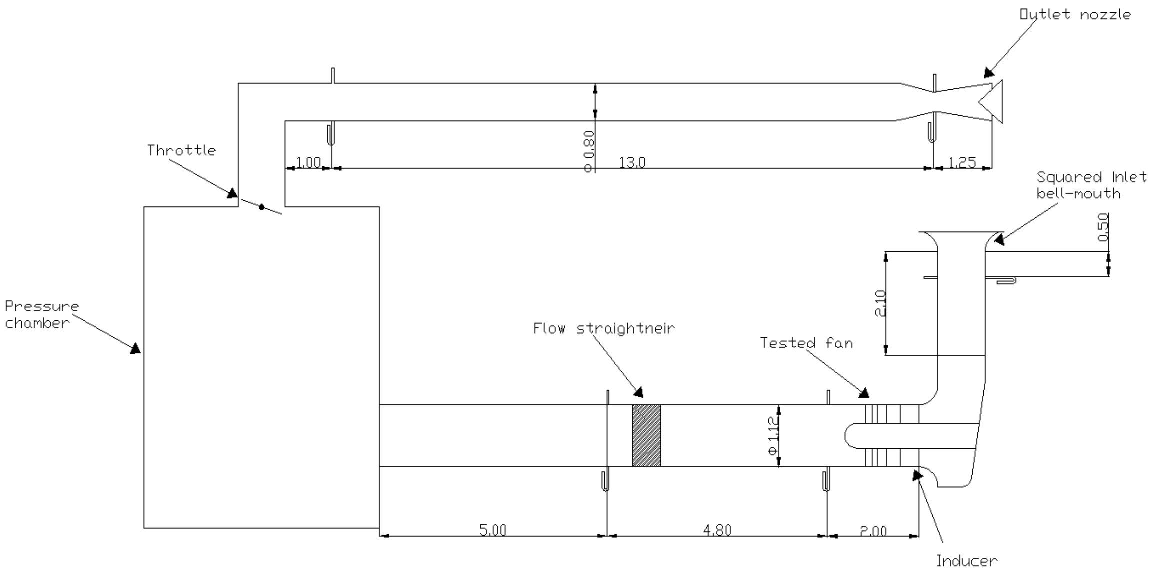

Fig. 1 Test rig set-up scheme (not to scale)

The duct which contained the fan, exhausted into a plenum chamber equipped with a throttling valve on the top of the chamber (Figure 1) in order to provide a mechanism for changing the fan pressure rise. A convergent-divergent NACA standard nozzle, instrumented for the measurement of

The measurements sessions have been carried out at the many different operating points, each measuring intervals lasted sixty seconds. The overall total pressure rise was computed from the average exit-area total pressure and average inlet-area total pressure. The accuracy of pressure measurements was ± 0.5% of measured data for all probes and pressure taps.

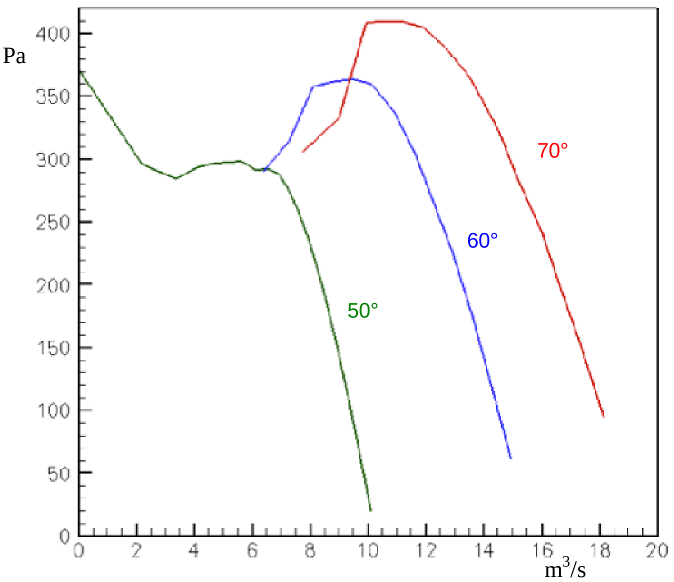

Fig. 2 Total pressure rise fan performance map

Casing instrumentation

The authors instrumented the fan rotor casing with two inserts, each containing a probe for unsteady pressure measurement. During the test, two microphones: B&K 4190, with sensitivity -26.2 dB re 1 V/Pa, monitored the wall pressure at the fan's casing. This sensors arrangement showed effectiveness in detecting a low speed fan's pressure behaviour [27].

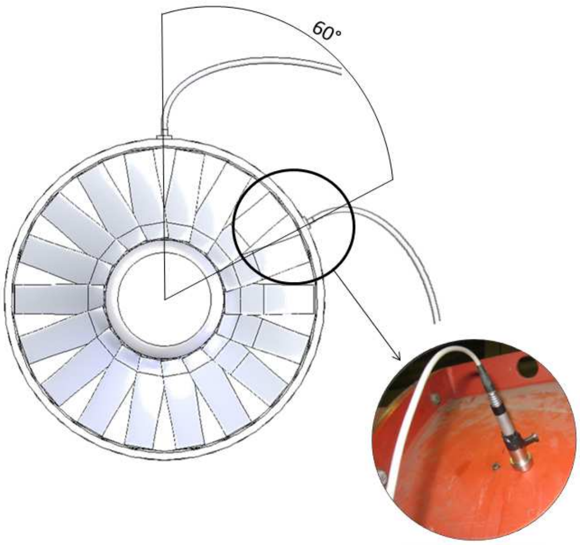

Fig. 3 Sectional view of the impeller with the microphones mounted flush with the casing wall

Tip leakage flow usually triggers the inception of rotating stall as one of the most critical three dimensional features. Nevertheless, since researchers believe that the developed stall cell consists of vortices in front of the rotor, a two dimensional consideration is essential in assessing the stall cell incipience and its behaviour. For this reason, the authors mounted the probes in the azimuthal disposition at half-chord distance from the block's leading edge.

Figure 3 shows the position of the microphones on the casing. The authors mounted each microphone on the fan case with an appropriate support (Figure 3) designed to guarantee the mechanical stability of the sensors during the dynamic tests. The authors used a charge amplifier to condition the microphones which sent the signal outputs to a digital data acquisition system (NI Compact Acq. 9172 with NI 9205 analogical input module) which displayed directly on a computer screen. The authors sampled each channel at a speed of 10 kHz. The complete duration of all the tests was about 120 s in order for the fan to throttle toward the stall region and then the VPIM to recover from this unsteady condition. The authors recorded and post processed all the data with a spatial and temporal cross-correlation with the method described below.

Figure 3 also shows the microphones mounted flush with the casing's inner wall with an angular anomaly (θ) of 60°. The authors mounted the fast-response sensors, each having a diameter of 15 mm, using a slight recess with a reduction of the sensing area (that is, diameter of 10 mm). Figure 3 shows the probe arrangement.

The range of uncertainty for readings was 0.1–0.2 dB at 1kHz, as given by the microphones' calibration certification and acquisition system according to ISO IEC60651 [25]. The authors estimated the error in pressure measurements, due to the turbulence, at 2% of the signal in accordance with the rotor casing's average turbulence level [28].

Signal processing technique

The authors used the microphones purely as pressure transducers to resolve high-frequency signals whilst maintaining good sensitivity. They recorded the measurements at a sampling rate of 10 kHz and measured the Nyquist frequency as f = 5 kHz.

To avoid signal aliasing, the authors preliminarily filtered all data at 2.5 kHz and analysed them in the range of interest below 200 Hz. The resulting Nyquist-rate (NR) was 1.2 kHz which was largely below the sampling frequency, thus verifying the second condition in the Nyquist problem on signal aliasing. Although flush mounted, the authors noted the presence of a small cavity in front of the microphones' diaphragm. The authors calculated the cavities' resonance frequency as f = 4702.11 Hz, using the Helmholtz equation applied to the equivalent conical cavity. They calculated the system frequency response using the *PreMeSys* 2.0 MatLab application tool, developed at the Von Karman Institute of Fluid Dynamics [29], to characterise the pressure measurement system's dynamic response under a step input signal.

The behaviour of the response suggested that limiting the signal analysis to 500 Hz would retain the cross spectrum amplitude in an unamplified region and the phase angle shift below – 3°.

The authors filtered the traces to remove high-frequency content and attenuate the blade-passing fluctuations. They used

150 Hz low-pass cut-off frequencies in this study in an attempt to detect rotating instabilities of relatively small magnitude. The authors accomplished filtering in post-processing using a non-causal digital filter which eliminated the phase distortion. This filtering technique gave an insight into the rotating features tracing the pressure signals prior to the stall initiation.

The authors estimated the overall uncertainty on unsteady pressure measurements as: (i) $\Delta V = 1000$ mV ± 12 mV (20:3) on the voltage and (ii) $\Delta G = 200$ dB ± 2.4 dB (20:3) on the raw signal gain in the range of considered frequencies. The authors were confident and accepted the uncertainty estimation due to the highly unstable characteristics of the investigated phenomena [30].

UNSTEADY MEASUREMENTS DURING THE STALL INCEPTION

The primary objectives of the measurements were: (i) to identify the nature of stall onset for the investigated fan when running at full speed and (ii) to characterise the rotating stall pattern in terms of the associated instabilities and their behaviours.

Visual inspection

Using the base-line technique, visual inspection of stall inception traces can provide qualitative information about the mechanism at play during the stall onset. This method remains essential to the study of stall. Customary for this analysis, the authors scaled and offset unsteady pressure histories from different locations around the rotor annulus on a single plot to produce an effect similar to a waterfall plot. The authors measured the unsteady fan behaviour at 100% of nominal speed (700 rpm).

Figure 4 shows the pressure traces low-pass filtered at 150 Hz as measured on the casing probes, whilst the authors throttled the fan from stable to stalled operations.

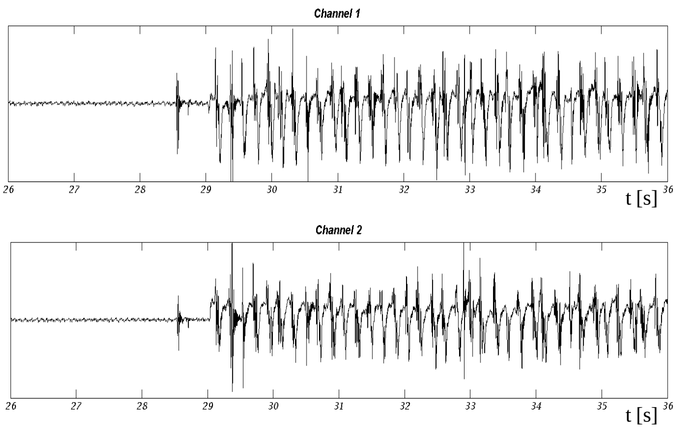

Fig. 4 Pressure time history for the two different probes flush mounted at the blade tip region

The authors drove the fan to stall within a time interval of 30 s. The pressure time traces in Figure 4 shows the evolution of this signal in a time interval of 36 s in order to highlight the dynamic of the transition from stable to unstable. Notably in Figure 4, the probes are arranged so that signals from the direction of rotation were bottom to top and the time is in seconds taken from the throttling start.

The authors did not notice modes in the pressure histories, Figure 4, but a more complex behaviour was apparent with the coexistence of rotating disturbances when they operated the fan at a higher operative point, i.e. after 28 s with the fan delivering a 410 Pa total pressure rise.

Channel 2 detected a spike-like pressure instability and then Channel 1 captured a similar signal. According to the relative position on time history *abscissae* in Figure 4, it was possible to compute that the pre-stall spike travelled at 70% of the rotor speed. The authors documented similar behaviour in a study on the spike-like pressure instability during the stall inception of a NASA37 compressor stage [31]. The peculiarity of the spike-like instability that the authors found in this study was the dynamics induced by this pressure peak. After the spike disturbance occurrence, the,pressure signal returned to the stable values for approximately 3 rotor revolutions. Whilst in Zhang *et al.* the spike-like instability immediately drove to stall [31], probably as a consequence of the diverse rotor shaft frequencies.

Figure 5 depicts the detail of the time sequence whilst the spike-like inception (I_1) drove the fan to a fully developed stall in about 2.5 s after its appearance at t = 28,5 s.

From Figure 5 it is possible to infer that the spike I_1 is followed by a second spike-like instability (I_2) rotating at 50% of the shaft speed. As observed above, the instability I_1 didn't drive directly to stall, but after the pressure perturbation producing that spike, associated with a probable instability at the blade tip, the pressure returned to a stable operation value and the successive pressure perturbation I_2 appeared after 0.5 seconds. I_2 featured a different shape closely related to the embryonic stage of a proper stall cell. Whilst I_1 was a time-concentrated single spike, I_2 appeared to cover a larger time length. The authors even observed a different waveform in the following pressure instabilities, namely I_3, I_4 and I_5.

In particular, the authors recognised the instabilities I_3 and I_5 as having the same wave structure as I_2, characterised by a pressure rise with a typical bow-shape, followed by multiple narrow peaks. The time lag of these peaks' occurrence was also similar to I_2, thus travelling at half of the rotor shaft speed. On the other hand, the I_4 instability kept the waveform shape and the rotational frequency observed in I_1.

Approaching t = 30 s, the pressure signal gave evidence of a new structure, called RS1, that the authors could consider the waveform of the new-born rotating stall cell. The authors then found the fully developed rotating stall cell, labelled RS6, after t = 31 s. This cell, resulting from the interaction among the set of faster pre-stall instabilities, moved at 40% of the rotor shaft speed. Day [32] documented similar 'unusual' stall patterns in a single stage compressor configuration as typical of the interaction among short-length-scale and long-length-scale cells.

Table 4 presents a summary of the rotating stall precursors and the developed rotating stall cell configurations.

The authors measured the amplitude of the pressure fluctuations representing instabilities which drove the fan to full stall condition, respectively fifteen (I_1) to fifty times (I_3) the pressure fluctuation amplitude during stable operation.

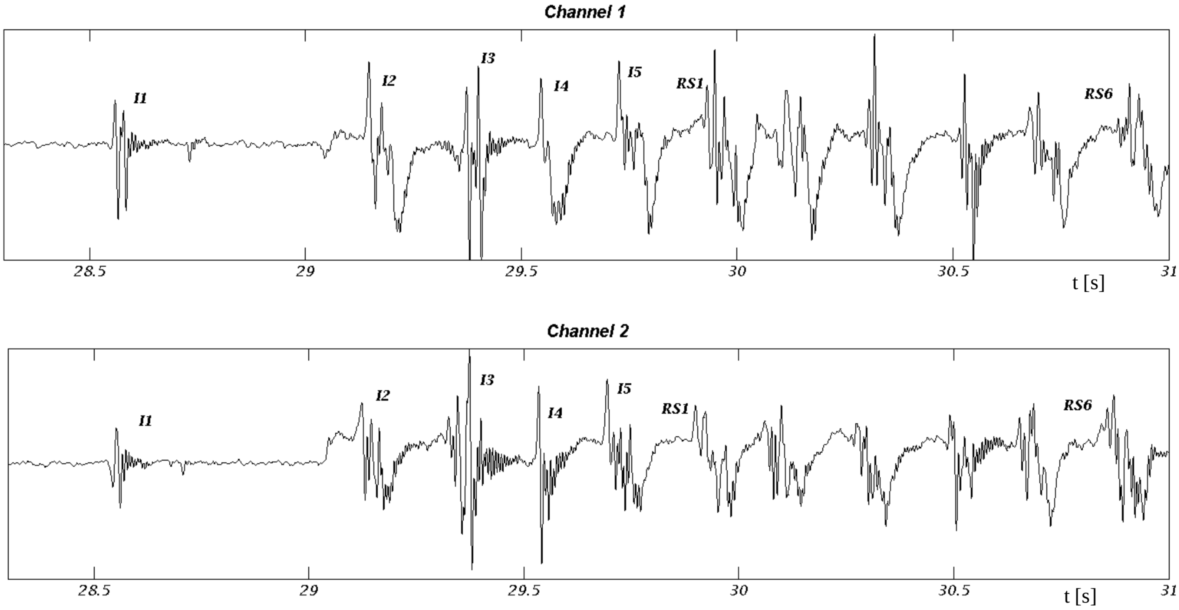

Fig. 5 Detail of time sequence during stall inception

Table 4 Stall precursors and rotating cell configurations

	Channel 1	Channel 2
Stall inception *I₁*		
Stall inception *I₂*	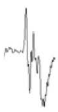	
Stall development *I₃*		
Stall development *I₄*		
Rotating stall *I₅* and *RS1*	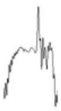	
Rotating stall *RS6*		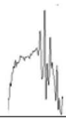

Outa [33] found similar complex aerodynamic features in the unsteady loads of the blade tip section in a single stage subsonic axial compressor. After a numerical investigation [33], Outa linked the cause of this phenomenon to a significant change of flow incidence inside the cell and to the presence of a retarded high pressure passage where the cell trailing edge vortices drive the incident flow to merge with the back flow at the blade leading edge region.

Accordingly, the authors could interpret the pressure instabilities isolated in Table 4 as indicative of the separation bubble inducing the pressure spikes during the inception and the vortices part of the stall cell with a multiple peaks structure. In general, during stall incipience, the leading instabilities at the blade's leading edge (I_1 and I_4) recess at their trailing side [33] and then form a vortex at their leading side which grows and merges into the preceding instability. A typical configuration of such a stall cell is the RS6, as Table 4 illustrates.

Multiple-spikes I_2, I_3 and I_5 appeared most frequently as precursors of full stall and their results were RS1 and then RS6 waveforms, whilst single-spike I_1 and I_4 were characteristic of the inception process. Figure 5 illustrates the multiple pressure spikes. This twin system induced light separation vortices in the blade passage that followed the pressure instability. After the instabilities drove to the full rotating stall cell, due to a significant reverse flow, the separation vortices ejected upstream and the leader vortex maintained its strength by accumulating the ejected vorticity. Such a developed vortex forced the high incident flow to turn with low incidence and almost one blade channel in the blade passages approached the cell region.

Spectral analysis

The authors substantiated the above pressure signal analysis using a Fourier analysis, which transformed the signal and provided information about the amplitudes of different oscillations. This enabled identification of frequency bands that better reveal the stall onset.

Figure 6 presents the cross spectra of the casing-wall pressure traces that the two sensors recorded simultaneously. The sampling period was 120 s, spanning from the peak flow rate condition to the stall event. The authors applied the FFT of the signals in a time window lasting 18 rotor revolutions, during the stable operation Δt = 10 s – 11.5 s (Figure 6.a), across the stall incipience Δt = 28.5 s – 30 s (Figure 6.b) and at full developed stall Δt = 50 s – 51.5 s (Figure 6.c). pre-stall precursors. Bianchi *et al.* [27] have recently confirmed the same findings in a subsonic axial fan.

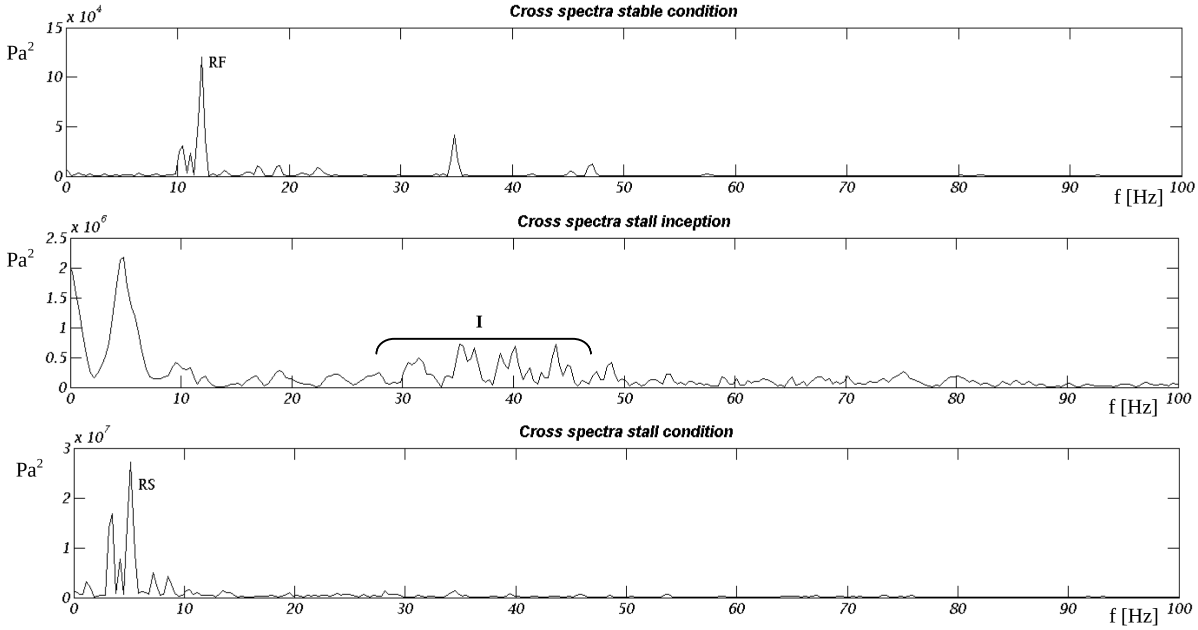

Fig. 6 Cross correlation spectral amplitude of the two pressure signal during a) the fan normal operations, b) the stall inception and c) during the stall event

When looking at the cross spectrum recorded in normal operation (Figure 6.a), the authors found that the presence of the shaft rotational frequency tone (RF), at 11.7 Hz, dominates the low frequency range. In contrast, when throttling the rotor to the peak pressure (Figure 6.b), the Fourier analysis highlighted a single, very low-frequency peak, indicative of the inception of rotating stall operation in agreement with results previously reported by Kameier and Neise [19] and by Bianchi *et al.* [27]. The authors identified this low-frequency peak by means of the spectral analysis in the frequency range 0 Hz to 10 Hz. Surprisingly, although the *spectrum* refers to a pre-stall behaviour, this low frequency tone featured a frequency close to that of the fully developed rotating stall cell.

The RF tone (i.e. 11.67 Hz), in Figure 8.b, became irrelevant when compared to RS. The authors interpreted the cancellation of this tone as the modulation of the shaft frequency rate *per* its interaction with other rotating instabilities in low speed axial turbomachinery [19, 27]. In light of this experimental evidence and in the vein of Kameier and Neise's [19] theoretical arguments, one can interpret the spikes as the trace of rotating sources of pressure fluctuations with a non-uniform circumferential distribution. Each spike corresponds to one spatial Fourier component which one can interpret as the rotational frequency of the corresponding source mechanism relative to the adopted fixed frame polar coordinate system. To this end, the authors could attribute the peak's frequency to an embryonic stall as already speculated in the visual inspection of

An interesting feature that the wall pressure spectra at stall incipience (Figure 6.b) revealed was the appearance of tone components at frequencies between 30 Hz and 50 Hz, labelled I in Figure 6.b. As noted by Bianchi *et al.* [27], the interaction of many small bubble cells created the stall cell, represented in this case by the global effect of the pressure instabilities, which are not strong enough to be revealed as fundamental tones in the cross spectrum amplitude, but appear as an increment of the broadband in the range of frequency where they exist.

Figure 6.c showed that the peak (RS6 in Figure 6.b) localised at 5 Hz split in a modulation of three pressure peaks during the stall event. These side bands group, labelled RS, were peculiar harmonics of the wall pressure spectra at fan stall [27].

The authors infer that, due to the aerodynamic characteristics of the studied fan rotor, the pressure disturbances borne as stall spots in the range of 30 to 50 Hz during the stall incipience, grew further, decreased their speed and merged with the spike-like stall cell located at 40% of the shaft rate. Others have reported similar observations under dynamic inflow distortion with tip injection [34] and in a similar axial fan [35]. Several small components initially formed the cell, which therefore rotated at highest speed, as described in the pressure signal's visual inspection. A few seconds after the incipience, the small stall cells evolved into a main unique cell (RS in Figure 6.c), resulting in a reduction of its rotational speed. The stall cell followed the feature exposed by Outa in the paper cited above [33] and by Bianchi *et al.* [27].

UNSTEADY MEASUREMENTS DURING THE STALL RECOVERY *VIA* VPIM BLADES

The objectives of the measurements in this second paragraph of the results were: (i) to characterise the transient rotating stall pattern, in terms of the associated instabilities and their behaviours, during the variation of blade pitch; and (ii) to identify the nature of stall recovery for the investigated fan when the VPIM system was in operation.

To the best of the authors' knowledge, the work reported in this paper is the first published study on stall inception and recovery by varying fan blade pitch angle at constant speed in a low-speed axial rotor. Despite the lack of published scholarly work against which to validate their conclusions, the authors have speculated on the stall recovery by studying the instantaneous pressure signals.

Figure 7 clearly illustrates the evolution in the pressure waveform. During the pitch motion, the waveform didn't change its amplitude.

The authors recognised two exceptions to this behaviour. The first was at t = 80 s after a blade rotation of about 7° that was marked by an isolated pressure peak followed by the phase shifting of the rotating stall cell period. The second exception, just before t = 84 s, was marked by an abrupt drop-off in Channel 1 pressure signal. Then, after t = 89 s, the recorded static pressure began to stabilise according to the hypothesis of a rotating stall recovery. Notwithstanding, it was difficult to infer an interpretation of the mechanism driving to the stall recovery from the pressure fluctuations survey given by the visual inspection in Figure 9 only.

For the sake of the clarity, Figure 8 presents the pressure waves in a period lasting 6 s before the stall's complete

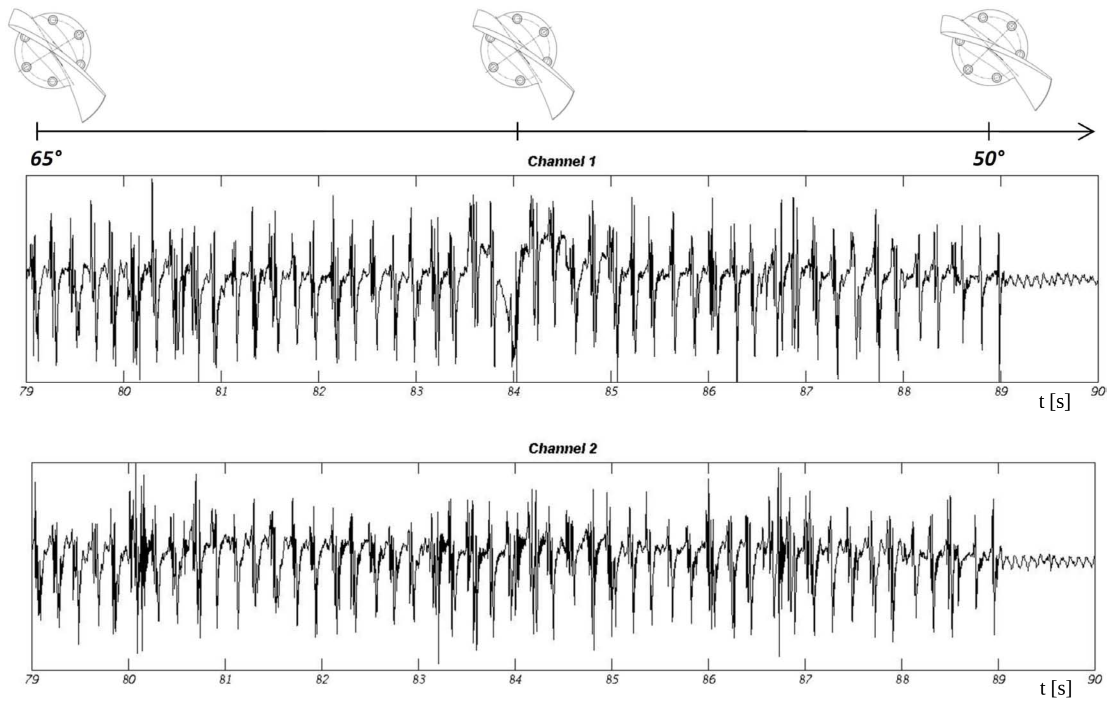

Fig. 7 Pressure time history for the two different probes flush mounted at the blade tip region

The authors carried out the transient by starting the blade pitch motion about t = 75 s (not shown in Figure 7), whilst the rotor was working under a rotating stall. They recovered a stable operating point after 14 s and a blade pitch angle variation of 20° at constant throttle position.

Visual inspections

Figure 9 shows the casing static pressure traces low-pass filtered at 150 Hz as measured on the two circumferential probes, whilst the authors kept the fan stalled and they operated VPIM to recover from stalled operations. The pressure traces focused on the operating region's time transient from the fully developed stall to normal operation recover. Figure 7 also shows the pitch angle axis, ranging from 65° to 50° during the last 10 s before stall suppression.

Figure 8 shows that, further reducing the pitch angle, the rotating stall cell waveform gradually changed its shape entailing a modification of the vortex configuration of the cell.

The authors selected the investigated time interval, with a 12° blade rotation, far enough (8,0 s after) from the time abscissa of VPIM actuation in order to account for the dynamics of fluid-to-blade interaction independently from the short-time effects correlated with the blade motion initiation. In examining the pressure signal during the blade motion transient, unexpectedly, the reduction of blade load consequent to the pitch adaptation didn't result in a remarkable variation of the measured pressure level in the leading edge region. On the contrary, the recorded signals appeared mostly influenced by the volume flow rate ingested by the rotor which was nearly constant during the VPIM driven stall recovery transient.

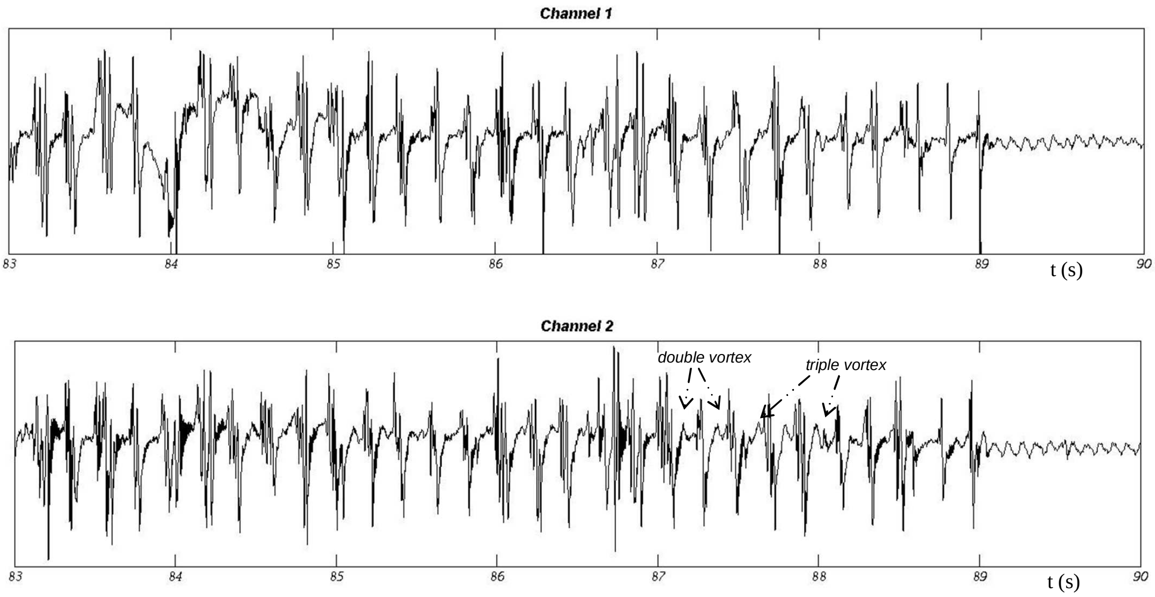

Fig. 8 Detail of the time sequence during the stall recovery

The peculiarities of the pressure time histories, Figure 8, stayed in contrast to the stall cell evolution as well as that of the correlated vortex structures driven by the competing effects of vortex merging and separation within the cell. This behaviour was clearly visible, focusing on the last 2 s before the stall suppression on Channel 2 signal, for instance. Notably, the typical waveform, signature of a fully developed single vortex type stall cell (i.e. RS6 in Figure 5) [33], evolved first in double vortex cell-like structure and then in a triple vortex cell. Stall cell frequency during the supposed vortex separation and merge sequence didn't change. At t = 89 s, after a blade angular motion of 20°, the blade recovered incidence conditions close to the aerodynamic optimum. This circumstance contributed to washing out abruptly a multiple vortex stall cell of reduced energy content.

Spectral analysis

The authors completed the study of the unsteady pressure measurements during the stall recovery with spectral analysis. To this end, their chosen metric was the evolution of signal spectral energy density because the visual inspection already suggested the stall cell's invariance of the frequency content during the transient. In particular, the integration of spectra was limited to the low frequency range, i.e. below 14 Hz, in order to cut-in only the effect of those structures related to the rotor shaft and the stall cell frequencies.

Figure 9 shows the evolution of the spectral energy density function, computed on the cross-spectra. In detail, Figure 9.a shows the overall variation during the transient lasting 155 s from stable condition to stall (throttle period) and the return to stable operation (VPIM period). Figure 9.b presents the evolution of the spectral energy density with the pitch motion to suppress during the transient (14 s) requested to recover from a stalled operation.

The evolution of the spectral energy density, Figure 9.a, confirmed that the appearance of the first spikes (I_1, I_2) caused a sharp discontinuity in the low freqency band energy content pushing it up to the level typical of a full stall behaviour. It also showed, from this specific metric viewpoint, that the stall incipience ended-up at t = 32 s. At full stall condition, the energy density appeared to oscillate about a well defined average level until the VPIM start-up. At t = 75 s, the pitch motion initiation immediately resulted in an abrupt energy density reduction of the computed cross spectra. This drop-off remarkably continued to extend until t = 89 s, when the VPIM actuation had rotated the blade pitch of 20°. With this, the authors could consider the abscissa that coincided with the time at which the pressure signals recovered the stable behaviour as the end of the transient during which the VPIM recovered from full stalled operation.

A close look at the stall recovery transient, which Figure 9.b illustrates, permitted the authors to speculate on the stall dynamics driven by the blade pitch motion. The region between t = 75 s and t = 89 s represented the transient under pitch motion.

Notably, the dynamics of stall suppression as *per* the spectral energy density featured three different patterns of decreasing energy content. During the first 8 s from the VPIM actuation (up to t = 83 s), the energy density decreased following a nearly linear descent halvening the energy density level. This behaviour was in accord with the blade loading reduction driven by the 12° pitch rotation. It is worth noting that, in contrast to the evidence that emerged from the pressure signal visual inspection, the spectral energy density immediately sensed the pitch motion. A second pattern was evident after t = 83 s, when the energy density distribution featured a plateau lasting about 4 s. Finally, during the last 2 s of the VPIM transient, the energy density abruptly dropped-off following a time evolution as fast as that of stall inception.

Concerning this pattern, it was possible to infer that the energy density fall was an indication of the on-going evolution in the stall cell configuration from single to multiple vortex cell.

REMARKS ON THE FAN PERFORMANCE CHART

The analyses of instantaneous pressure measurements on the casing wall permitted the isolation of safe and stalled operation regions and both the performance curve path during the VPIM operation's (Figure 10) transient.

The VPIM drove the fan across its performance curve at standard pitch angle and effectively recovered the stall when the pitch angle best matched with the flow incidence at about 50° of hub pitch.

During the stall recovery transient, the fan rotor experienced a de-rating of the pressure rise capability about 28% of the stalled level whilst the ingested volume flow had a 16% reduction.

CONCLUSIONS

The present study has established the stall characteristic of a subsonic axial fan by visual inspection of the pressure traces and acoustic correlations from two different pressure probes mounted on the casing. The authors have investigated both the nature of stall conditions for the tested rotor and the characteristics of the stall-instability precursors with the fan driven towards stall at customary blade pitch angle.

The first stage of the investigation utilised visual inspection to characterise the fan's behaviour when driven to stall.

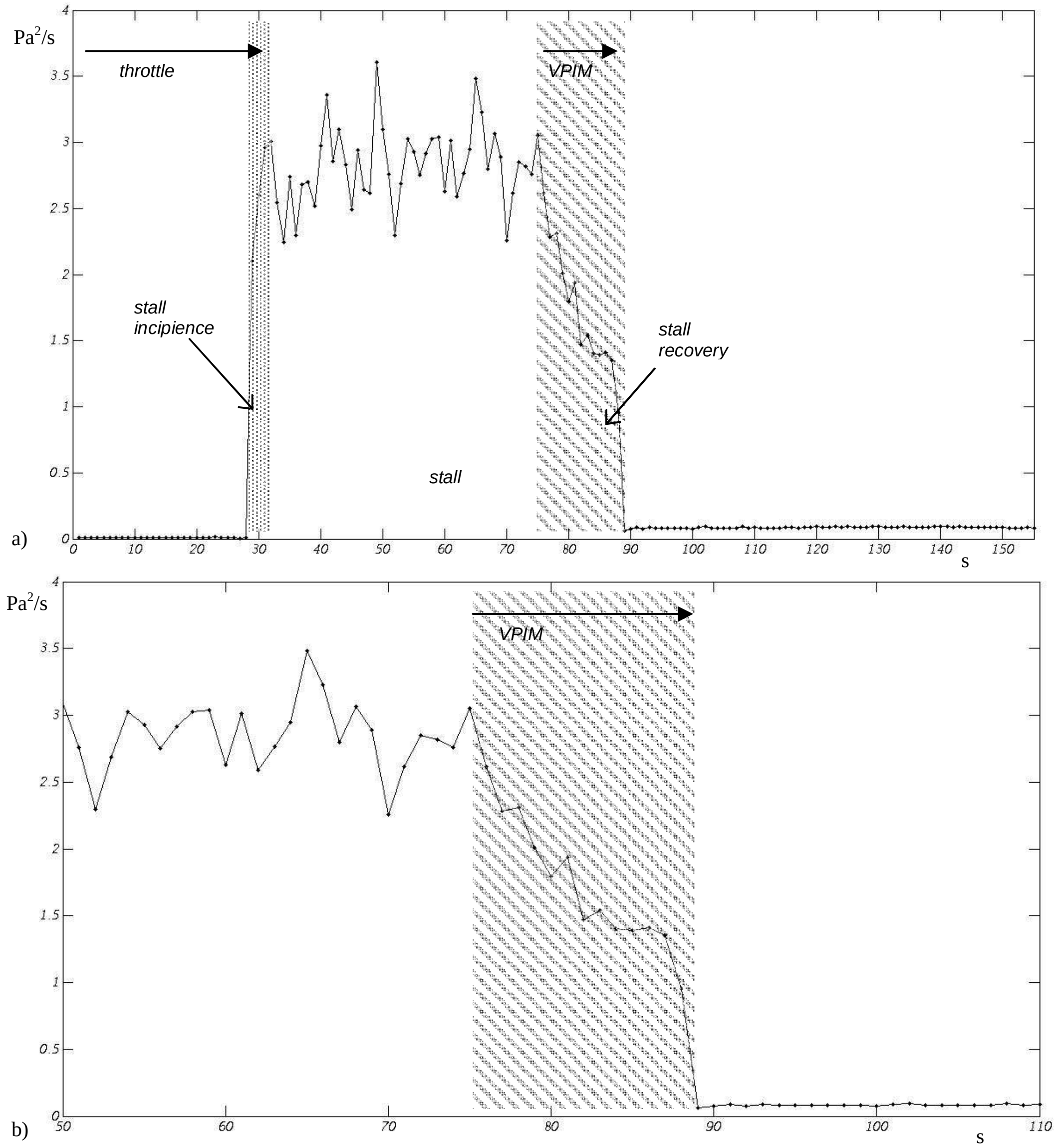

Fig. 9 Spectral energy density of wall pressure: a) overall evolution, and b) stall recovery transient

The fan exploits peculiar stall patterns. At the nominal shaft rate and pitch angle, the authors found that the fan stall evolves within a few revolutions after its inception featuring an interaction between rotating cells moving at different speeds.

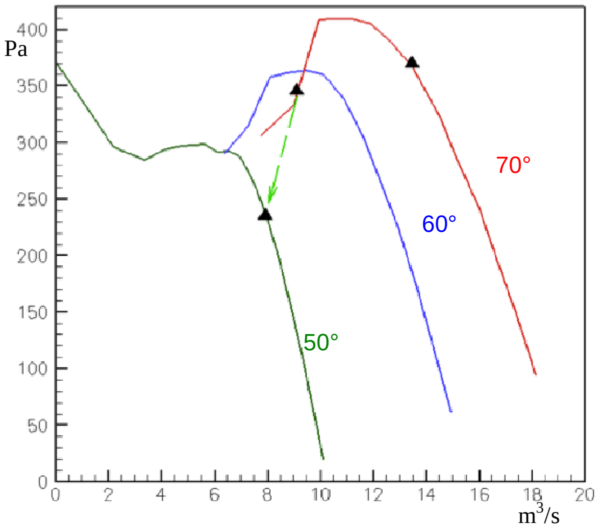

Fig. 10 Fan Performance Chart after the stall recovery by VPIM blades

The Fourier transformation of cross-correlated pressure signals from different azimuthal positions provided more detailed information about the tested fan rotor's stall behaviour. The spectral analysis that the authors conducted when the throttle position caused the inception of pressure instabilities, detected the presence of a low frequency tone component related to rotating stall. The tone-band modulations also recognised the harmonics due to the interaction of different weak pressure instabilities before the stall event. The authors could conclude the existence of a single cell rotating stall's signature in this fan type.

Despite these observations, traditional fan and compressor stall-warning systems are unable to utilise the spectrum of measured pressure alone to predict the imminent onset of stall because the required long sampling time precludes its use in practice. As such, an alternative approach to stall warning is required to enable stall precursor utilisation in identifying stall onset. Because the fan that the authors used in these experiments shows a peculiar behaviour in the pre-stall, lasting about one second, this finding provides helpful points for those setting up a stall warning system. Moreover, the work presented recently by Sheard et al [36] may provide some insight into understanding the spike-like instability which procured the proper stall in the quickest reaction time and also the back reaction to the stall recovery when a VPIM system is at work.

To the best of the authors' knowledge, the work they report in this paper is the first published study on stall inception and recovery by varying fan blade pitch angle at constant speed in any axial turbomachinery. The potential of a variable pitch constant speed fan stall recovery system, operated to extend a fan's stable operating range beyond that which one classically associates with a fixed pitch variable speed fan, could be extended in a "joint control system" used together with the rotational speed. The key point is that an engine control system can have direct control over the blade pitch in a variable pitch fan, but can only have indirect control over the speed of a fixed pitch variable speed fan.

ACKNOWLEDGMENTS

Fläkt Woods Group and the Dipartimento di Meccanica e Aeronautica, "Sapienza" University of Rome undertook the present research in the context of the contract FW-DMA09-11. The authors thank Fläkt Woods AB, Växjö, for the use of its facility in this project. Two of the authors (Bianchi and Corsini) acknowledge the assistance of MIUR (the Italian Ministry for Academic Research) under the projects *Ateneo Federato AST.* Bianchi and Mazzucco acknowledge the help of Dr. H. Trigesson and M. Olof Karlsson during their work at Fläkt Woods AB.

REFERENCES

[1] Greitzer, E., M., 1980, "Review - Axial compressor stall phenomena", Journal of Fluids Engineering, **102**, pp. 134-151.

[2] Day, I., J., and Cumpsty, N.A., 1978, "The measurement and interpretation of flow within rotating stall cells in axial compressors", Journal of Mechanical Engineering Science. **20**, pp. 101-114.

[3] Moore, F.,K., 1984, "A Theory of Rotating Stall of Multistage Compressors, Parts I-III", ASME J. of Engineering for Power, **106**, pp.313-336.

[4] Emmons, H.,W., Pearson, C.,E., and Grant, H.,P., 1955, "Compressor surge and stall propagation", Transactions of the ASME, **77**, pp. 455–469.

[5] Gravdahl, J.,T., and O., Egeland, 1999, Compressor surge and rotating stall: Modeling and control, Springer Verlag, London.

[6] Cumpsty, N., A., 1989, "Part-circumference casing treatment and the effect on compressor stall", ASME Paper 89-GT.

[7] Rippl, A., 1995, "Experimentelle Untersuchungen zuminstationaren Betriebsverhahen an der Stabilitarsgrenze eines mehrstufigen transsonischen Verdichters", PhD Dissertation, Ruhr-Universitat Bochum.

[8] Sheard, A.G. & Corsini, A. 2011, 'The Impact of an Anti-Stall Stabilisation Ring on Industrial Fan Performance: Implications for Fan Selection'; Proceedings of the 55th American Society of Mechanical Engineers Turbine and Aeroengine Congress, Vancouver, Canada, 6–10 June, Paper No. GT2011-45187.

[9] Corsini, A., Minotti, S., Sciulli, F., Sheard A. G., 2009, "The role of computational methods in the development of an aero-acoustic design methodology: application to a family of large industrial fans", *14th Conference on Modelling Fluid Flows*, Budapest, HU.

[10] Sheard, A.G., and Jones, N.M. 2008, "Approval of high-temperature emergency tunnel-ventilation fans: the impact

of ISO 21927-3", *Proceedings of the ITA-AITEES World Tunnel Congress and 34th General Assembly*, Agra, India.
[11] EN12101-3, 2002, Smoke and heat control systems. Specification for powered smoke and heat exhaust ventilators.
[12] ISO 21927-3, 2006, Smoke and heat control systems - Part 3: Specification for powered smoke and heat exhaust ventilators.
[13] Camp, T.R., and Day, I.J., 1998, "A study of spike and modal stall phenomena in a low-speed axial compressor", J. of Turbomachinery, **120**, pp. 393-401.
[14] Vo, H. D., Tan, C.S., Greitzer E.M., 2005, "Criteria for spike initiated rotating stall", ASME paper GT2005-68374.
[15] Deppe, A., Saathoff, H., Stark, U., 2005: "Spike-type stall inception in Axial Flow Compressors", 6th Conference on Turbomachinery, Fluid Dynamics and Thermodynamics, Lille, France.
[16] Bright, M., M., Qammar, H., Vhora, H., Schaffer, M., 1998, "Rotating Pip Detection and Stall Warning in High-Speed Compressors Using Structure Function", Proceedings of AGARD RTO AVT Conference.
[17] Okada, K., 1987, "Experiences with flow-induced vibration and low frequency noise due to rotating stall of centrifugal fan", Journal of low frequency noise & vibration, **6**(2), pp. 76-87.
[18] Mongeau, L., Thompson, D.E., McLaughlin, D.K., 1995, "A method for characterizing aerodynamic sound sources in turbomachines", J. of Sound and Vibration, **18**(3), pp. 369-389.
[19] Kameier F., and Neise W., 1997, "Rotating blade flow instability as a source of noise in axial turbomachines", Journal of Sound and Vibration, **203**, pp. 833-853.
[20] General Electric Company (Cincinnati, OH), 1975, "Fan with variables pitch blades and translating bearing attuation system" US Patent References 2648387.
[21] Flakt Woods Online Catalog, http://www.flaktwoods.com/.
[22] Langston, Lee, S., 2009, "Fitting a pitch"ASME Mechanical Engineering Magazine, **131**(12), pp. 38-42
[24] ISO 5801, 2007, Industrial fans - Performance testing using standardized airways.
[25] ISO IEC60651, 1994, Specification for sound level meters.
[26] Greitzer, E., M., 1976, "Surge and Rotating Stall in Axial Flow Compressors, Part I: Theoretical Compression System Model,", ASME J. Eng. for Power, **98**, pp. 190-198.
[27] Bianchi S, Sheard, AG, Corsini A & Rispoli F, Detection of Stall Regions in a low Speed Axial Fan. Part I-Azimuthal Acoustic Measurements , Proceedings of the 55th American Society of Mechanical Engineers "Gas Turbine and Aeroengine Congress", Paper No. GT2010-22753, Glasgow, UK, June 6th – 10th, 2010.
[28] Corsini, A., Rispoli, F., 2005, "Flow analyses in a high-pressure axial ventilation fan with a non-linear eddy-viscosity closure", Int. Journal of Heat and Fluid Flow, 26(3), pp. 349-361.
[29] Boerrigter, H., L., 1996, "PreMeSys: A simulation program to determine the frequency and time response of a pressure measurement system", VKI Technical Memorandum.
[30] Carbonaro M., *et al*, 2009, "Measurement Techniques in Fluid Dynamics - An Introduction", Von Karman Institute for Fluid Dynamics, Rhode Saint Genèse, Belgium, ISBN: D-1994-0238-417
[31] H. W. Zhang, X. Y. Deng, F. Lin, J. Y. Chen, W. G. Huang, 2005, 'Unsteady tip leakage flow in an isolated axial compressor rotor' J. Therm. Sci. **14** (3), pp. 265-274
[32] Day, I.J., 1993, "Stall inception in axial flow compressors", Journal of Turbomachinery, **115**, pp. 1-9.
[33] Outa E., 2005, "Rotating stall and stall-controlled performance of a single stage subsonic axial compressor", J. Therm. Sci. **15** (1), pp. 1-13
[34] Leinhos, D. C., Schmid, N. R., and Fottner, L., 2001, "The Influence of Transient Inlet Distortions on the Instability Inception of a Low Pressure Compressor in a Turbofan Engine", Journal of Turbomachinery, **123**, pp. 1–8.
[35] McDougall, N., M., Cumpsty, N., A., Hynes, T., P., 1990, "Stall inception in axial compressors", Journal of Turbomachinery, **112**, pp. 116-123.
[36] Sheard A G, Corsini A, Bianchi S, "Stall Warning in Low Speed Axial Fan by Visualization of Sound Signal", accepted on Journal of Engineering for Gas Turbines and Power, manuscript reference number GTP-10-1168